

Longitudinal and Transverse Spin Responses in Relativistic Many Body Theory

K. Yoshida and H. Toki

Research Center for Nuclear Physics (RCNP), Osaka University, Ibraki, Osaka
567-0047, Japan

Abstract

We study theoretically the spin response functions using the relativistic many body theory. The spin response functions in the relativistic theory are reduced largely from the ones of the non-relativistic theory. This happens particularly to the longitudinal spin responses. This fact is able to remove the difficulty in reproducing the ratio of the longitudinal and transverse response functions seen experimentally. We use the local density approximation with the eikonal approximation to the nuclear absorption on the incoming and outgoing nucleons for the calculations of the response functions of finite nuclei. We compare the calculated results with the recent experimental results with $(p;n)$ reactions on C and Ca.

PACS : 24.10.Jv, 24.70.+s, 25.40.Kv

keywords : spin response function, relativistic many-body theory, quasielastic reaction

1 Introduction

The spin response functions are very interesting, since they convey directly the informations on the spin correlations among nucleons. The longitudinal spin responses are related with the pionic correlations, which have a strong connection with pion condensation and its precritical phenomenon [1, 2]. The transverse responses are related with the rho mesonic correlations. Due to the mass difference between the pion and the rho meson, the meson exchange force is attractive in the pion channel while it is repulsive in the rho meson channel at medium momenta, $q \sim 2 \text{ fm}^{-1}$. Hence the comparison of the two spin responses should reflect this feature directly. In fact, the ratio between the spin responses in these channels was predicted to be largely different from unity [3].

Experiments on the spin responses were performed at LAMPF and RCNP at intermediate energies following the above ideas in mind [4, 5]. The experimental results were found, however, extremely puzzling. The ratios of the longitudinal and the transverse spin responses for various nuclei were found close to or less than one, which is largely different from the theoretical expectations [4, 6]. The surface effects were considered by Esbensen et al., but the ratio could be brought down only to a factor two [7]. Very involved calculations were performed by Ichimura et al. by considering the finite nuclear geometry and the realistic distortion effects [8]. The results were essentially unchanged from that of Esbensen et al.

These results indicate that something essential is missing in the spin correlations among nucleons in nuclei. In this respect, there was a very interesting observation made by several authors [9, 10]. With the use of the pseudovector coupling of the pion with the nucleon instead of the pseudoscalar coupling in the relativistic framework, the pion response becomes much weaker than that of the non-relativistic framework. The pion response function is reduced by a factor $(M \rightarrow M)^2$ and the effective mass, M^* , reduces largely in nuclear matter as the density increases in the relativistic many-body theory [11, 12, 13, 14]. Hence, even at the normal matter density without the Landau-Migdal short range correlations, i.e., $g^0 = 0$, the pion condensation does not occur. This is a very interesting observation, since this fact largely reflects in the longitudinal spin response, which is the pion response, and it could be the source to remove the discrepancy.

Horowitz and his collaborators are the ones who apply this idea to the spin response functions and the various spin observables [10]. They found that in fact the ratio could be brought down to close to one in accordance with the experimental observations. These calculations were performed in nuclear matter assuming some typical density representing the nucleus of interest. In this paper, we would like to take into account the change of the densities by considering the hadron distortion effects and compare with the experimental data. In doing so, we would like to compare our results not only with the ratios of the spin responses, but also with the response functions themselves. Particularly, we would like to compare with the recent intensive experimental studies of the $(p;n)$ reactions at 400 MeV by H. Sakai and his collaborators [6].

This paper consists of the following contents. We write the definition of the response functions and the expressions of the spin response functions in the relativistic framework in Sect.2. We provide the numerical results in Sect.3, where we demonstrate the effects of the relativity on the spin response functions both for the longitudinal and the transverse channels at different densities. We choose here the matter properties calculated by the relativistic mean field theory (RMF) with the non-linear terms with the parameter set TM1 [15]. Sect.4 is devoted with the summary of this work.

2 Spin response functions

Spin response functions extracted from quasielastic $(p;p^0)$ and $(p;n)$ reactions have been described by $\chi + g^0$ model which attributes spin dependent interaction in a nucleus to NN and NN residual force [16]. The spin dependent responses contain the longitudinal and transverse components with respect to momentum transfer q . In the non-relativistic model the longitudinal response comes from χ channel with vertex q and the transverse one from χ channel with vertex q . The relativistic version of the model follows Walecka model [11] with spin dependent interaction Lagrangian [13]

$$L_{int} = \frac{f}{m} \bar{\psi} \gamma_5 \psi \partial_\mu \phi + g_N \bar{\psi} \gamma_\mu \psi \partial_\mu \phi + \frac{g_N}{2M} \bar{\psi} \gamma_\mu \psi \partial_\mu \phi + \dots \quad (1)$$

M is the nucleon mass and $\kappa = 6.6$ is the tensor-to-vector ratio in the NN coupling [17]. As for NN channel, pseudovector coupling is favored from theoretical

points of view [18]. The first analysis of the spin response with this model was done by Horowitz et al., who calculated spin transfer observables [10]. Our goal is to reveal relativistic effects directly from Lindhard response functions considering nuclear distortion effect and reproduce the experimental cross section observed in $(p;n)$ reactions on finite nuclei. In the lowest order the spin dependent excitation is described in terms of polarization functions by the interaction with 4-momentum transfer $q = (\omega; \mathbf{q})$ between the incident and the outgoing nucleons. For nuclear matter

$$i_{PV}(q) = \text{Tr} \int \frac{d^4k}{(2\pi)^4} \gamma_5 \mathbf{q} \cdot \mathbf{1} G(k+q) \gamma_5 \mathbf{q} \cdot \mathbf{2} G(k) \quad (2)$$

$$i_{\parallel}(q) = \text{Tr} \int \frac{d^4k}{(2\pi)^4} \mathbf{1} G(k+q) \mathbf{2} G(k) \quad (3)$$

where $\mathbf{1} = \frac{\mathbf{q}}{2M} \cdot \mathbf{q}$ ($\mathbf{2} = \mathbf{1} + \frac{\mathbf{q}}{2M} \cdot \mathbf{q}$). $G(k)$ is Hartree nucleon Green's function,

$$\begin{aligned} G(k) &= G_F(k) + G_D(k) \\ G_F(k) &= (\mathbf{k} + M) g_F(k); \quad G_D(k) = (\mathbf{k} + M) g_D(k) \\ g_F(k) &= \frac{1}{k^2 - M^2 + i}; \quad g_D = \frac{i}{k} \cdot \mathbf{k}_0 \cdot \mathbf{k} \cdot (\mathbf{F} \cdot \mathbf{k}_0) \\ \mathbf{k} &= \frac{(\mathbf{k}_0 \cdot \mathbf{v}; k)}{q} \\ k &= k^2 + M^2; \end{aligned}$$

F denotes the Fermi energy $F = \sqrt{k_F^2 + M^2}$ with k_F the Fermi momentum. $M = M + \sigma$ is nucleon effective mass given by relativistic Hartree theory with $\sigma; \mathbf{v}$ scalar and vector potential. The transverse polarization \mathbf{T} is obtained by projecting onto the plane perpendicular to \mathbf{q} [19]. Thus

$$\begin{aligned} \mathbf{L} &= \mathbf{PV} \\ \mathbf{T} &= \left(\frac{q_0^2}{q^2} \mathbf{00} + \frac{\mathbf{i}}{i} \right) = 2; \end{aligned} \quad (4)$$

We neglect the divergent vacuum polarization $\int \frac{d^4k}{(2\pi)^4} G_F G_F$ which represents NN coupling.

$i_{PV}(q)$ is written as [20]

$$i_{PV} = 16M^2 q^2 \int \frac{d^4k}{(2\pi)^4} g(k) g(k+q) \quad (5)$$

where $g(k) = g_F(k) + g_D(k)$. On the way to come to Eq.(5), we have used the vector current conservation relation, $\mathbf{q} \cdot \mathbf{j} = 0$. Eq.(5) is given by $I_0(q)$ in [21].

$$\text{Im} i_{PV} = \frac{M^2 q^2}{|\mathbf{q}|^2} \int \int_{\mathbf{k}} \begin{cases} \mathbf{k} \cdot \mathbf{j} < k_F \\ \mathbf{k} \cdot \mathbf{j} > k_F \end{cases} \begin{cases} \mathbf{k}_+ < k_F \\ \mathbf{k}_- < k_+ \end{cases} \quad (6)$$

$$\text{Re } \epsilon_L = \frac{M^2 q^2}{j^2 j} \left(\ln \frac{(k_F + k_+) (k_F - k_-)}{(k_F + k_+) (k_F + k_-)} - 2 \ln \frac{k_F + k_F}{M} \right) + \ln \frac{(M^2 + k_+ k_F - k_+ k_F) (k_F + k_+)}{(M^2 - k_+ k_F - k_+ k_F) (k_F - k_+)} + (k_+ - k_-) \quad (7)$$

$$k = \frac{j^2 j}{2} \left[1 - \frac{4M^2}{q^2} \right] \quad (8)$$

The explicit form of ϵ_T is written in [21], where the response functions in ($e; e^0$) inelastic scattering were calculated.

To define response function in the relativistic model, it is necessary to consider non-relativistic limit of the vertex operators since all the discussions have been made in the non-relativistic framework. While $\epsilon \ll q \ll \epsilon_F$,

$$\frac{i}{2M} \epsilon \ll \frac{+1}{2M} \epsilon \quad (9)$$

Thus we define the relativistic response functions R_L, R_T by

$$q^2 R_L = \frac{1}{\epsilon} \text{Im } \epsilon_L \quad (10)$$

$$\frac{+1}{2M} \epsilon^2 q^2 R_T = \frac{1}{\epsilon} \text{Im } \epsilon_T \quad (11)$$

They correspond to the polarization functions in non-relativistic model R_{NR}

$$q^2 R_{NR} = \frac{1}{\epsilon} \text{Im } \epsilon_{NR} \quad (12)$$

where ϵ_{NR} is the non-relativistic polarization function by vertex operators, $\epsilon \ll q$ or

$q \ll \epsilon$. In the non-relativistic model the longitudinal response and the transverse response agree with each other for the nuclear matter and they are expressed by the Lindhard function given in [22]. Here we would like to compare the longitudinal response functions in the relativistic model and the non-relativistic model. First in the high density case, k_F is large and hence the large region of response function is given by the ϵ term in Eq.(6). A typical case is shown in Fig.1. In this region

(low ϵ region), $R_L = \frac{M}{M^2} R_{NR}$. Second in the low density case, k_F is small and hence the contribution from the ϵ term in Eq.(6) is limited to the very small ϵ as seen in Fig.2. Hence, we want to figure out where the response function becomes maximum. Seeing the second term in Eq.(6), it is obvious that the peak appears for $k = 0$. This corresponds to the excitation energy, $\epsilon = \sqrt{q^2 + M^2} - M$ from Eq.(8). In this case we find $\text{Im } \epsilon_L = \frac{M^2 q^2}{j^2 j} \left(\frac{M}{M} \right) = \frac{M k_F^2 q^2}{2 j^2 j}$. On the other

hand, in the non-relativistic case the peak position is $\epsilon = \frac{q^2}{2M}$ and the peak height is $\text{Im } \epsilon_{NR} = \frac{M k_F^2 q^2}{2 j^2 j}$. This implies that the relativistic responses are reduced by a factor $\frac{M}{M^2}$ at the higher density and by $\frac{M}{M}$ at the lower density compared with the non-relativistic one at the same density. Obvious comparison is difficult in the transverse case due to the more complicated expression for the relativistic case.

The correction by introducing χ and χ exchange interaction is carried out by the random phase approximation. RPA is done by summing up ring diagrams to all orders and expressed by Dyson's equation

$$\chi^{RPA} = \chi^0 + \chi^0 V \chi^{RPA} \quad (13)$$

χ^0 is the free response function defined above and χ^{RPA} is the full response function obtained by RPA. For the meson channel they carry Lorentz indices which is not explicitly shown. V is χ and χ meson exchange interaction

$$V(\mathbf{q}) = \frac{f^2}{m} \frac{1}{q^2 - m^2} \frac{g^0}{q^2} \quad (14)$$

$$V(\mathbf{q}) = g^2 (g - \mathbf{q} \cdot \mathbf{q} / m^2) \frac{1}{q^2 - m^2} C \frac{g^0}{q^2} \quad (15)$$

$C = 2.18$ is the ratio of couplings of non-relativistic interactions $\frac{f^2}{m^2} = \frac{f}{m}^2$ and g^0 and g^0 are phenomenological Landau-Migdal parameters introduced to take into account short range nuclear correlations. Considering $\mathbf{q} = 0$ and decomposition,

$\chi = P^L \chi_L + P^T \chi_T$, where $P^{L,T}$ are projection operators which extract the longitudinal and transverse part $\chi_{L,T}$ for the meson channel [19], the RPA response functions are written in a simple form,

$$\chi_L^{RPA} = (1 - V \chi_L^0)^{-1} \chi_L^0 \quad (16)$$

$$\chi_T^{RPA} = (1 - V \chi_T^0)^{-1} \chi_T^0 \quad (17)$$

with

$$V(\mathbf{q}) = g^2 \frac{1}{q^2 - m^2} C \frac{g^0}{q^2} \quad (18)$$

We take $g = 2.6$ which satisfies

$$\frac{f}{m} = g \frac{+1}{2M} \quad (19)$$

The Landau-Migdal parameter was originally introduced in the non-relativistic χ and χ model and in that case $g^0 = g^0$, since

$$\begin{aligned} V_{g^0} &= g^0 \frac{f^2}{m} \frac{1}{q^2 - m^2} \frac{1}{q^2} \\ &= g^0 \frac{f^2}{m} \frac{1}{q^2 - m^2} \frac{1}{q^2} + \frac{f^2}{m} C \frac{1}{q^2 - m^2} \frac{1}{q^2} \end{aligned} \quad (20)$$

$g^0 = 0.6 - 0.7$ is usually used as a standard value. On the other hand in the relativistic model g^0 and g^0 may be different from each other because of the absence of such a constraint as Eq.(20). Horowitz et al. found that the free response calculated for finite nuclei reproduces $(e; e^0)$ data at $q = 1.7 \text{ fm}^{-1}$ and chose $g^0 = 0.3$ which minimizes the

effect of RPA correlations [10]. As for g^0 we have no information so far and we shall take the conventional value, $g^0 = 0.7$. Thus we use the parameter set $g^0 = 0.3; g^0 = 0.7$.

It is noted that the relativistic response is reduced by $\frac{M}{M^*}$, which causes also the coupling polarization effects reduced by the same factor effectively. At the lower density, on the other hand, the factor $(M^* = M) (k_F = k_F^0)^2$ reduces again the coupling effectively, where $k_F^0 = 1.36 \text{ fm}^{-1}$ is the Fermi momentum at the normal density.

In (p, n) reactions the distortion effect is of much importance compared with (e, e^0) reaction. Due to large nucleon-nucleon cross section σ_{NN} the reaction takes place at the nuclear surface rather than in the central region. In order to take into account this effect we carry out the calculation of the (p, n) cross sections under the local density approximation. Attenuation factor at $(b; z)$ in the cylindrical coordinate, with the incident nucleon coming from $z = -1$ and the outgoing nucleon going away to $z = +1$, is defined by $e^{-\chi(b)}$ where $\chi(b) = \int_{-1}^{+1} dz \sigma_{NN}(b; z)$. Then the response function for finite nucleus is expressed by

$$R^{LDA} = \frac{1}{N_e} \frac{N}{A} \int_{-1}^{+1} dz \int_0^{\infty} db db dz e^{-\chi(b)} (b; z) R(k_F) \quad (21)$$

Effective neutron number N_e is given as normalization factor

$$\begin{aligned} N_e &= \frac{N}{A} \int_{-1}^{+1} dz \int_0^{\infty} db db dz e^{-\chi(b)} (b; z) \\ &= \frac{N}{A} \frac{1}{\sigma_{NN}} \int_{-1}^{+1} dz \int_0^{\infty} db db (b) e^{-\chi(b)} \end{aligned} \quad (22)$$

Here the appearance of the $\frac{N}{A}$ factor is to use the neutron density instead of nucleon density in Eq.(21),(22). For the nuclear density $\rho(r)$ we adopt the three-parameter Fermi-type form determined experimentally [23]. The response function R is obtained at each $(b; z)$ through the density $\rho(b; z)$ with the help of the relativistic mean field calculation for nuclear matter [14]. We use $\sigma_{NN} = 30 \text{ mb}$ which is close to the free cross section at the relevant energy $T_{lab} = 400 \text{ MeV}$. Typical Fermi momentum k_F is defined by replacing $R(b; z)$ in Eq. (21) by $k_F^{-1=3}$. $k_F = 0.98 (0.97)$ for ^{12}C (^{40}Ca). M^* for the density is $M^* = 0.82 (0.83) M$.

3 Numerical results

Throughout this section we show the results for the reactions with $q \approx 1.7 \text{ fm}^{-1}$ which are of special interest in this problem and measured by the experiments. To begin with we will demonstrate relativistic effects on free response functions of nuclear matter at different densities. In Fig.1 we show the free response functions for the symmetric nuclear matter at the normal density $k_F = 1.36 \text{ fm}^{-1}$, with the effective mass $M^* = 0.59M$ which is given by RMF calculation. For comparison the non-relativistic response function and the relativistic response with $M^* = M$ are also shown in the figure. We see that the longitudinal spin response R_L with $M^* = 0.59M$ is suppressed from the non-relativistic response due to the effect of the effective mass. This is affirmed by seeing that R_L becomes close to R_{NR} setting $M^* = M$. As stated in

the previous section they agree with each other for $\theta < 30^\circ$. Consequently, there appears broadening of the width because of enlarged maximum particle-hole excitation energy for given momentum transfer $(k_F + j)^2 + M^2 - k_F^2 + M^2 - \frac{k_F j}{M}$. The transverse response R_T also shows the similar effective mass dependence. However it is larger than the longitudinal response with the same effective mass. This more moderate dependence of R_T on the effective mass comes from the complex structure of NN coupling vertex which contains the vector and the tensor terms. As a result $R_L = R_T = 0.8$ with little dependence on θ . In Fig.2 the free response functions for $k_F = 0.97 \text{ fm}^{-1}$ ($M = 0.83$) are shown. It corresponds to the density $\rho = 0.37 \rho_0$. ($\rho; \eta$) reaction takes places in the surface region of nucleus with about this density because of the large distortion of the incident and outgoing nucleon. The width becomes narrower and the magnitude becomes higher than at the normal density due to the larger effective mass. The qualitative features in the previous figure also hold true here. At this density the relativistic response is reduced by the factor $\frac{M}{M^*}$ rather than $\frac{M}{M^*}^2$. The difference between R_L and R_T is also smaller than Fig.1. It makes $R_L = R_T = 0.94$. In any case $R_L = R_T < 1$ holds in the relativistic case. This fact is important to reproduce the experimental observation $R_L = R_T = 1$.

Next we show relativistic effects on the responses calculated by RPA. In Fig.3 (a) we show the longitudinal responses with RPA at the normal density together with free response and non-relativistic results. We see that the relativistic response with RPA correlation R_L^{RPA} is only slightly enhanced by the attractive exchange interaction while the non-relativistic one is largely enhanced. The difference from the non-relativistic case comes from the effective coupling reduced by the factor $\frac{M}{M^*}^2$ which makes R_L^{RPA} closer to the free response, $R_L^{\text{RPA}} = R_L^{\text{free}}$. In Fig.3 (b) we show the transverse responses at the same density. It is found that the relativistic response with RPA R_T^{RPA} almost agrees with the free response. This is because $V = 0$ with $g^0 = 0.3$, while the non-relativistic response is much quenched by the repulsive exchange force with $g^0 = 0.7$. We find that the free longitudinal response reduced by the use of the relativistic expression as compared to the transverse response is compensated by the RPA correlation. It follows that $R_L = R_T = 1$ at low θ (Fig.5). It is in good contrast with the non-relativistic case where the longitudinal response exceeds significantly the transverse one. In Fig.4 (a), (b) we show the responses with RPA at $k_F = 0.97 \text{ fm}^{-1}$. The dependence of R^{free} on k_F causes the attractive exchange force weaker in both the non-relativistic and relativistic cases. In the latter case the factor $\frac{M}{M^*}$ reduces still more the interaction. As for the transverse response R_T^{RPA} agrees again with the free response. We obtain the ratio $R_L = R_T = 1.12$ at low θ , while the non-relativistic case results in $R_L = R_T > 2$ with striking θ dependence. The relativistic results are in agreement with the experimental situation in question.

Finally we compare the result obtained by the local density approximation with the experimental data recently measured at RCNP [6]. Fig.6 shows the results on ^{12}C (the left panels) and ^{40}Ca (the right panels). The in-medium cross section $\sigma_{NN} = 30 \text{ mb}$ provides effective neutron number $N_e = 2.0(3.7)$ for ^{12}C (^{40}Ca). Since the effective nucleon number we obtain differs from the experimental one, we multiply $N_e^{\text{exp}} = N_e$ to the experimental data where N_e^{exp} is the effective neutron number adopted in the

experimental analysis, $N_e^{\text{exp}} = 2.7(6.0)$ for ^{12}C and ^{40}Ca , respectively. This is because the "experimental" response functions extracted from the cross sections and the polarization measurements by the experimentalists were obtained by dividing the corresponding quantities with N_e^{exp} [4, 6]. On the other hand, the "theoretical" response functions are obtained by dividing the corresponding quantities with N_e as shown in Eq.(21). As seen in above discussion about the matter properties, the longitudinal and the transverse response are very close to each other. The theoretical results reproduce the experimental data at $\omega < 50\text{ MeV}$, above which 2-step process and excitation contribute to the response. As for the ratio (lower panels of Fig.6) the theory predicts $R_L/R_T \approx 1.12$ in agreement with the common experimental understanding that $R_L/R_T \approx 1$ although this overestimates slightly the new experimental data.

4 Conclusion

We have studied the relativistic effects on the spin response functions by using the relativistic version of the $\sigma + \rho$ model. We have calculated the polarization functions in the σ channel and ρ meson channel in the nuclear medium to obtain the spin response functions. We have adopted the pseudovector coupling for σ NN channel instead of the pseudoscalar coupling. The longitudinal response calculated by the pseudovector coupling is largely reduced by the effective mass which is $\frac{M^*}{M} = 0.6 - 0.8$ in the nuclear medium. The reduction factor is $\frac{M^*}{M}^2$ at the higher density and $\frac{M^*}{M}$ at the lower density. We have found that without RPA the longitudinal response is less than the transverse response even at the low density.

The effects of the effective mass also reduce effectively the coupling of σ NN and ρ NN in the medium. We have demonstrated that the relativistic longitudinal response function is much less enhanced than the non-relativistic one by the attractive exchange force. The transverse response with RPA correlation has been calculated with the Landau-Migdal parameter $g^0 = 0.3$, which is chosen by Horowitz et al. as a fitting parameter in the analysis of electron scattering. We have shown the transverse response is hardly affected by RPA. As a result we obtained similar response functions for the longitudinal and the transverse spin responses. It is in agreement with the experimental data which is contradictory to the non-relativistic theoretical calculation. The Landau-Migdal parameters in the relativistic model are not well established so far. More theoretical research in both nucleon-nucleon interaction and many-body phenomena as our work is needed to determine them definitely.

We have performed the local density approximation in order to take into account the nuclear distortion effect in $(p;n)$ reactions and the finiteness of a nucleus with the actual density distribution. Our results have reproduced the experimental data newly measured at RCNP at low ω region. The ratio of the longitudinal and the transverse response proved to be about unity, in agreement with the common experimental understanding.

Acknowledgment

We are grateful to H. Sakai, T. Wakasa, M. Fujiwara and I. Tanihata for fruitful discussions on the experimental aspects of (p,n) reactions.

References

- [1] A.B. Migdal, Rev. Mod. Phys. 50 (1978)107 and references therein.
- [2] H. Toki and W. Weise, Phys. Rev. Lett. 42 (1979)1034.
- [3] W.M. Alberico, M. Ericson and A. Molinari, Nucl. Phys. A 379 (1982)429.
- [4] T.A. Carey, K.W. Jones, J.B. McClelland, J.M. Moss, L.B. Rees, N. Tanaka and A.D. Bacher, Phys. Rev. Lett. 53 (1984)144.
L.B. Rees, J.M. Moss, T.A. Carey, K.W. Jones, J.B. McClelland, N. Tanaka, A.D. Bacher and H. Esbensen, Phys. Rev. C 34 (1986)627.
J.B. McClelland et al, Phys. Rev. Lett. 69 (1992)582.
X.Y. Chen et al, Phys. Rev. C 47 (1993)2159.
T.N. Taddeucci et al, Phys. Rev. Lett. 73 (1994)3516.
- [5] H. Sakai, M.B. Greenfield, K. Hatanaka, S. Ishida, N. Koori, H. Okamura, A. Okihana, H. Otsu, N. Sakamoto, Y. Satou, T. Uesaka and T. Wakasa, Nucl. Phys. A 577 (1994)111c.
- [6] T. Wakasa et al, submitted to Phys. Rev. C.
T. Wakasa, private communication.
- [7] H. Esbensen, H. Toki and G. Bertsch, Phys. Rev. C 31 (1985)1816.
- [8] M. Ichimura, K. Kawahigashi, T.S. Jørgensen and C. Gaarde, Phys. Rev. C 39 (1989)1446.
- [9] B.L. Bibrain, V.N. Fomenko and L.N. Savushkin, J. Phys. G 8 (1982)1517.
- [10] C.J. Horowitz and J. Piekarewicz, Phys. Lett. B 301 (1993)321.
C.J. Horowitz and J. Piekarewicz, Phys. Rev. C 50 (1994)2540.
- [11] J.D. Walecka, Ann. Phys. 83 (1974)491.
- [12] B.D. Serot and J.D. Walecka, Adv. in Nucl. Phys. 16 (1986).
- [13] R. Brockmann and R. Machleidt, Phys. Rev. C 42 (1990)1965.
- [14] D. Hirata, H. Toki, T. Watabe, I. Tanihata and B.V. Carlson, Phys. Rev. C 44 (1991)1467.
- [15] Y. Sugahara and H. Toki, Nucl. Phys. A 579 (1994)557.
- [16] E. Oset, H. Toki and W. Weise, Phys. Rep. 83 (1982)281.

- [17] G .H ohler and E .P ietarinen, Nucl. Phys. B 95 (1975)210.
- [18] T .M atsui and B D .Serot, Ann. Phys. 144 (1982)107.
- [19] H .Shiom i and T .H atsuda, Phys.Lett. B 334 (1994)281.
- [20] J.F .D aw son and J.P iekarew icz, Phys. Rev. C 43 (1991)2631.
- [21] H .K urasawa and T .Suzuki, Nucl. Phys. A 445 (1985)685.
- [22] A L. Fetter and J D . W alecka, Quantum theory of many-particle system s
(M cG raw-H ill, New York, 1971).
- [23] C W . de Jager, H . de Vries and C . de Vries, At. Data Nucl. Data Tables
14 (1974)479.

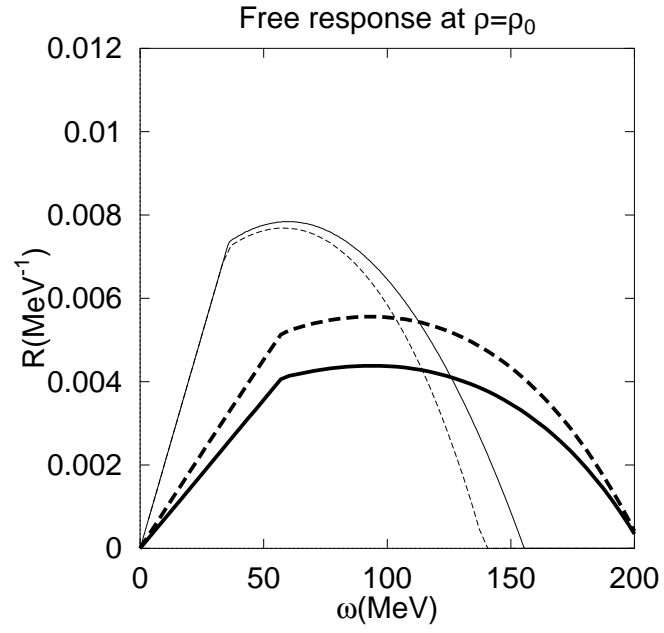


Figure 1: Free relativistic longitudinal response function R_L (thick solid curve) and transverse response function R_T (thick dashed) and non-relativistic one R_{NR} (thin solid) at $|\mathbf{q}| = 1.7 \text{ fm}^{-1}$ for the symmetric nuclear matter at the normal density $k_F = 1.36 \text{ fm}^{-1}$. For comparison relativistic longitudinal response with $M = M$ is shown (thin dashed).

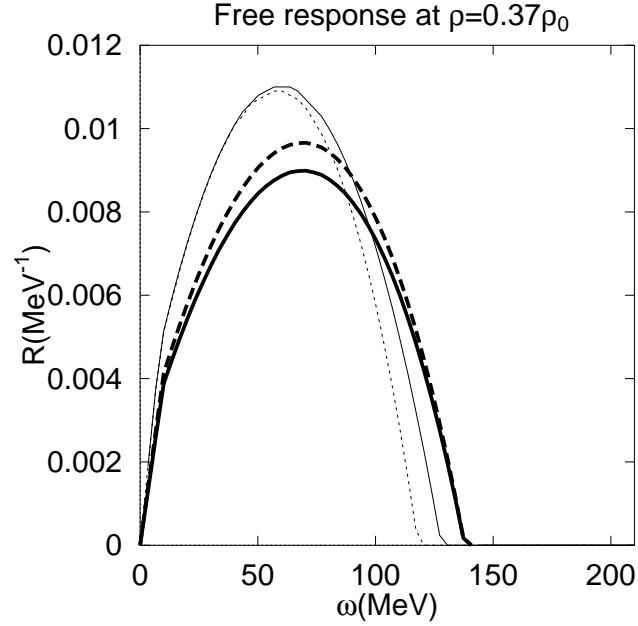


Figure 2: Same as Fig.1 for $k_F = 0.97 \text{ fm}^{-1}$ which corresponds to the typical density of the nucleus in $(p;n)$ reaction because of the large distortion of the incident and outgoing nucleons.

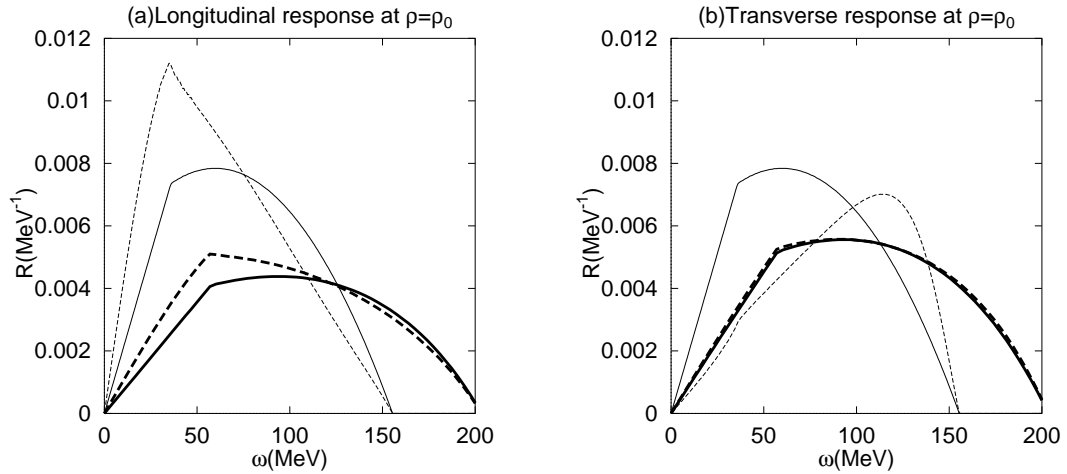


Figure 3: (a) Longitudinal and (b) transverse responses with and without RPA correlation at the normal density. Thick solid curves indicate the relativistic free responses R_L^{free} and R_T^{free} and thick dashed curves RPA results R_L^{RPA} and R_T^{RPA} . The corresponding non-relativistic values are drawn with thin solid and dashed curves.

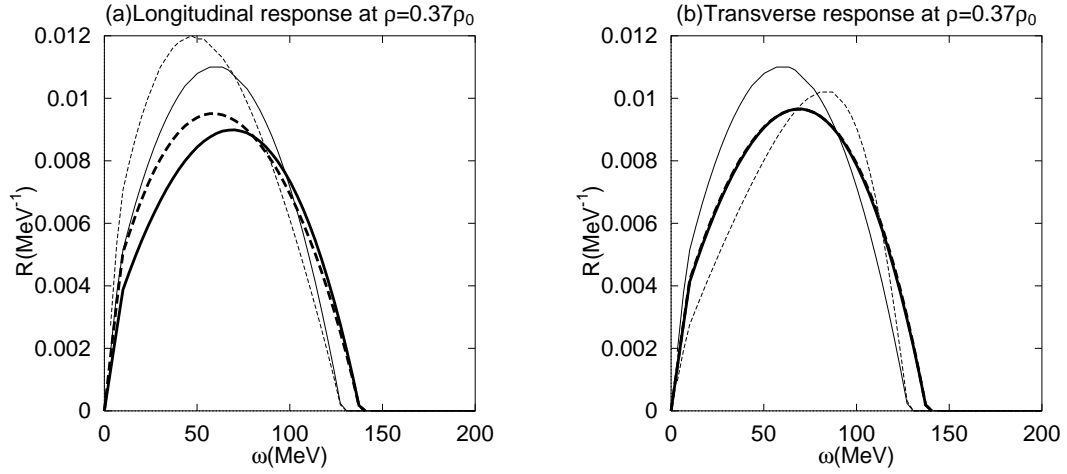


Figure 4: Same as Figure 3 for $k_F = 0.97 \text{ fm}^{-1}$.

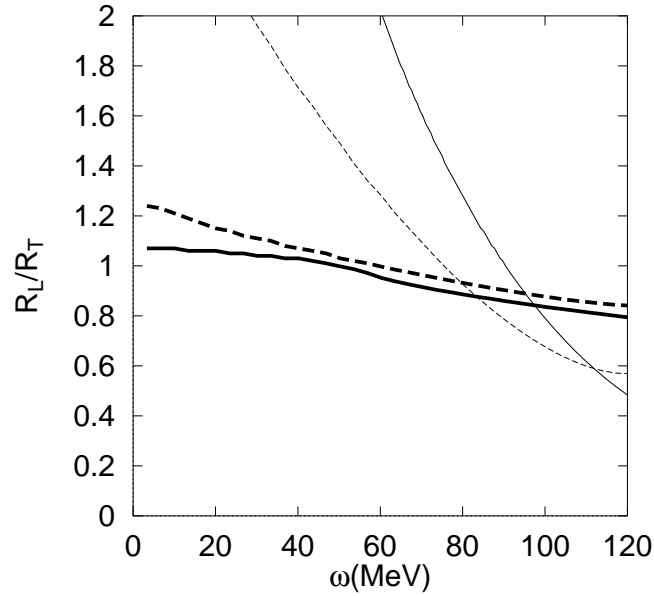


Figure 5: Ratio of the longitudinal response to the transverse one with RPA at the normal density and $k_F = 0.97 \text{ fm}^{-1}$ corresponding to $\rho = 0.37 \rho_0$. A thick solid curve indicates the relativistic result at the normal density and a thick dashed curve for $k_F = 0.97 \text{ fm}^{-1}$. Thin solid and dashed curves indicate the non-relativistic results at the normal density and at $\rho = 0.37 \rho_0$, respectively.

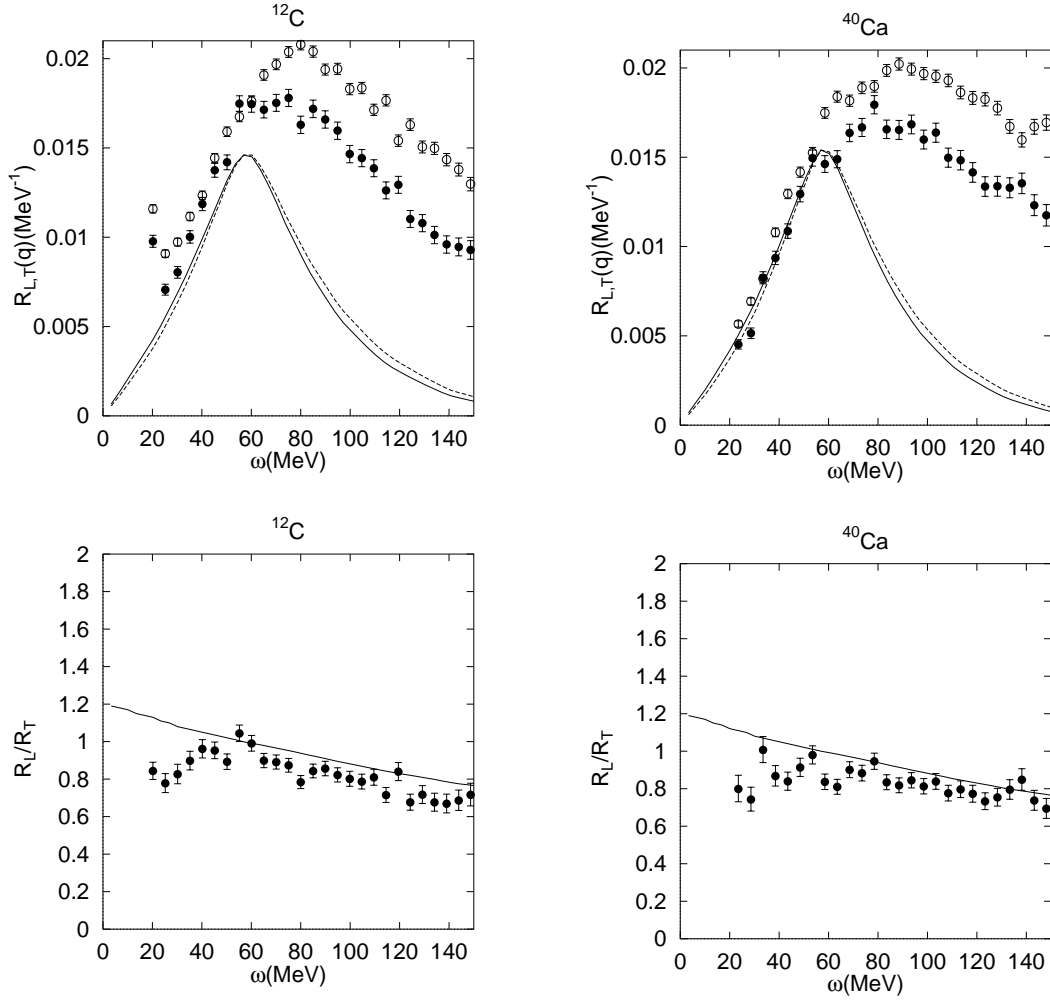


Figure 6: Response functions with RPA (upper panels) and ratio of the longitudinal to the transverse response (lower panels) at $|\mathbf{q}| = 1.7 \text{ fm}^{-1}$ obtained by the local density approximation with $N_{NN} = 30 \text{ mb}$ for ^{12}C (left panels) and ^{40}Ca (right panels). In the upper panels the longitudinal response is drawn by a solid curve and the transverse by a dashed curve. The experimental data are plotted by solid circles for the longitudinal response and by open circles for the transverse one. The experimental responses are multiplied by a factor $N_e^{\text{exp}} = N_e$ (see the text). In the lower panels the theoretical value is drawn in a solid curve and the experimental data are plotted by solid circles.